Kirk-Othmer Encyclopedia of Chemical Technology.

SIMULTANEOUS HEAT AND MASS TRANSFER

Heat transfer and mass transfer occur simultaneously whenever a transfer operation involves a change in phase or a chemical reaction. Of these two situations, only the first is considered herein because in reacting systems the complications of chemical reaction mechanisms and pathways are usually primary. Even in processes involving phase changes, design is frequently based on the heat-transfer process alone; mass transfer is presumed to add no complications. But in fact mass transfer effects do influence and can even limit the process rate.

In processes where a condensing vapor or vapor from a liquid phase moves through an inert gas, eg, condensation in the presence of air, drying, humidification, crystallization (qv), and boiling of a multicomponent liquid, mass-transfer as well as heat-transfer effects are important (see Air conditioning; Distillation; Evaporation). Such processes are discussed elsewhere in the *Encyclopedia*, but the primary emphasis is on either the heat transfer or the mass transfer taking place. Herein the interactions between heat and mass transfer in such processes are discussed, and applications to humidification, dehumidification, and water cooling are developed. These same principles are applicable to other operations.

1. Condensation and Vaporization as Effected by Simultaneous Heat and Mass Transfer

Consider the interphase transfer that occurs when one or more components change phase in the presence of inert or less active components. The transferring component must be transported through its original phase to the boundary, and must then escape into the second phase. The phase change involves a heat effect. Energy is transported to or from the boundary to balance the phase-change heat effect. The boundary temperature is influenced by the rate of heat transfer, and this determines the fugacity of the diffusing component at the boundary. Thus, to describe the process, rate equations for heat transfer and mass transfer must be written along with material balances for the components present and an energy balance. Appropriate boundary conditions must be applied, and the resulting set of differential and algebraic equations solved. The rate equations for heat and mass transfer express the rate of transport in terms of the driving force divided by the resistance across the transfer path. For heat transfer the driving force is expressed as a temperature difference, whereas the resistance is the reciprocal of the transport area times a coefficient. Here the concentration driving force should be a fugacity or activity difference with the coefficient in consistent units. However, these properties are not directly measurable so the driving force is expressed in terms of mole fractions, partial pressures, or mole ratios. The use of these terms requires the use of consistent coefficient values and limits the usefulness of the equations to systems that obey Raoult's law, or requires the use of empirical nonideality coefficients. Herein it is assumed that Raoult's law holds.

This process has been used for various situations (1–14). For the condensation of a single component from a binary gas mixture, the gas-stream sensible heat and mass-transfer equations for a differential condenser section take the following forms:

$$G{\cdot}C_p \frac{dT_G}{dA} = -h_g{\cdot}\left(T_g - T_s\right) \frac{\epsilon}{e^{\epsilon} - 1} \qquad (1)$$

$$\frac{dV}{dA} = -k_g \cdot \left(P_g - P_s\right) \qquad (2)$$

No condensation is taking place here in the bulk gas phase. If condensation does take place so that fogging occurs, these equations become

$$G \cdot C_p \frac{dT_G}{dA} = -h_g\left(T_g - T_s\right) \frac{\epsilon}{e^{\epsilon} - 1} + \lambda \frac{dF}{dA} \qquad (3)$$

$$\frac{dV}{dA} = -k_g\left(P_g - P_s\right) - \frac{dF}{dA} \qquad (4)$$

The term $\epsilon/(e^{\epsilon} - 1)$, which appears in equations 1 and 2, was first developed to account for the sensible heat transferred by the diffusing vapor (1). The quantity ϵ represents the group $M_i \cdot C_{pi}/h_g$, the ratio of total transported energy to convective heat transfer. Thus it may be thought of as the fractional influence of mass transfer on the heat-transfer process. The last term of equation 3 is the latent heat contributed to the gas phase by the fog formation. The vapor loss from the gas phase through both surface and gas-phase condensation can be related to the partial pressure of the condensing vapor by using Dalton's law and a differential material balance.

The effect on the coolant temperature of latent and sensible heat transferred to the surface from the condensing vapor is as shown in equation 5:

$$L \cdot M_L \cdot C_w \frac{dT_w}{dA} = \pm h_o \cdot (s - T_w) \qquad (5)$$

where the $\pm$ sign is negative for countercurrent flow.

Assuming a linear relation between surface temperature and corresponding vapor pressure of the condensable component allows a heat balance to be written from gas phase to the surface:

$$h_o \cdot (T_s - T_w) = h_g\left(T_g - T_s\right) \frac{\epsilon}{1 - e^{\epsilon}} + k_g \cdot \lambda \left(P_g - P_s\right) \qquad (6)$$

Combining equation 6 with the heat- and mass-transfer rate expressions gives

$$w \cdot C_w \frac{dT_w}{dA} = e^{\epsilon} \cdot G \cdot C_p \frac{dT_g}{dA} + \frac{V' \cdot \lambda P}{\left(P_t - P_{go}\right)\ \left(P_t - P_{gf}\right)} \cdot \frac{dP_g}{dA} \qquad (7)$$

Equations 6 and 7 are not affected by fogging because the latent heat thus obtained is retained as sensible heat in the gas phase.

These basic relations have been solved for a wide range of cooler–condenser conditions and for different complexities of systems. A design procedure based on the assumption that the mixture is saturated throughout the condensation process has been developed (2). This assumption was later shown to depend on the rate of diffusion of the condensing component: some cases having rapidly diffusing components tend to superheat, and others having slowly diffusing vapors tend to subcool. The same approach extended to superheated mixtures has been used to develop the following equation for calculating T and partial pressures, P, during condensation (3):

$$\frac{dP_g}{dT_g} = \frac{P_t - P_g}{(Le)^{2/3} \cdot P_{\mathrm{BM}}} \cdot \frac{P_g - P_s}{T_g - T_s} \cdot \frac{e^{\epsilon - 1}}{\epsilon} \qquad (8)$$

This relation was tested experimentally for water condensation in various gases and found to be acceptable (4). It has also been solved via analog computers (5), and in another instance, for a set of conditions ranging from

superheating to fogging (6). The use of standard *j*-factor correlations (see also Heat-exchange technology, heat transfer) for coefficients of heat and mass transfer have been incorporated into the solution method (4, 7, 8). Experimental verification has been supplied by workers in the field of absorption (qv) (9–11), condensation (12, 13), liquid–liquid extraction (see Extraction, liquid–liquid) (8, 14), and distillation (qv) (15), and in laboratory experiments where free convection played a significant role (15, 16).

In considering the effect of mass transfer on the boiling of a multicomponent mixture, both the boiling mechanism and the driving force for transport must be examined (17–20). Moreover, the process is strongly influenced by the effects of convective flow on the boundary layer. In Reference 20 both effects have been taken into consideration to obtain a general correlation based on mechanistic reasoning that fits all available data within $\pm 15\%$.

The boiling mechanism can conveniently be divided into macroscopic and microscopic mechanisms. The macroscopic mechanism is associated with the heat transfer affected by the bulk movement of the vapor and liquid. The microscopic mechanism is that involved in the nucleation, growth, and departure of gas bubbles from the vaporization site. Both of these mechanistic steps are affected by mass transfer.

The final correlation for the overall boiling heat-transfer coefficient in pipes or channels (20) is a direct addition of the macroscopic (mac) and microscopic (mic) contributions to the coefficient:

$$h_T = h_{\text{mac}} + h_{\text{mic}}$$

$$= \left[0.023\left(Re_{L-\text{only}}\right)^{0.8}(Pr_L)^{0.4}\,\frac{k_L}{D_i}\right]\left[\frac{(\frac{dP}{dz})_{2\phi}}{(\frac{dP}{dz})_{L-\text{only}}}\right]^{0.444} f(Pr_L)\left[\frac{\Delta\tilde{T}}{\Delta T_s}\right]_{\text{mac}}$$

$$+\ 0.00122\,\frac{k_L^{0.79}\cdot C_{P_L}^{0.45}\cdot\rho_L^{0.49}\cdot g_c^{0.25}}{\sigma^{0.5}\mu_L^{0.29}\lambda^{0.24}\rho_V^{0.24}}\,\Delta T_s^{0.24}\cdot\Delta P_s^{0.75}\cdot S_{\text{binary}}\cdot Re_{2\phi} \qquad (9)$$

where

$$f(Pr_L) = \left[\frac{Pr_L + 1}{2}\right]^{0.444} \qquad (10)$$

$$\left(\frac{\Delta\tilde{T}}{\Delta T_s}\right)_{\text{mac}} = 1 - \frac{(1-y_j)\,q}{\rho_{\text{avg}}\lambda k_Y \Delta T_s}\cdot\frac{\Delta T_s}{\Delta x_{jP_B}} \qquad (11)$$

$$k_Y = 0.023\left(Re_{2\phi}\right)^{0.8}\cdot(S_c)^{0.4}\,\frac{k_L}{D}$$

$$Re_{2\phi} = Re_{L-\text{only}}\left[f(Pr_L)\left[\frac{(\frac{dP}{dz})_{2\phi}}{(\frac{dP}{dz})_{L-\text{only}}}\right]^{0.444}\right]^{1.25} \qquad (12)$$

$$S_{\text{binary}}\cdot Re_{2\phi} = \frac{1}{1 - \frac{C_{PL}(y_j - x_j)}{\lambda}\cdot\frac{\partial T}{\partial x_j}\left[\frac{\alpha}{D}\right]^{1/2}}\,S\cdot Re_{2\phi} \qquad (13)$$

In the macroscopic heat-transfer term of equation 9, the first group in brackets represents the usual Dittus-Boelter equation for heat-transfer coefficients. The second bracket is the ratio of frictional pressure drop per unit length for two-phase flow to that for liquid phase alone. The Prandtl-number function is an empirical correction term. The final bracket is the ratio of the binary macroscopic heat-transfer coefficient to

the heat-transfer coefficient that would be calculated for a pure fluid with properties identical to those of the fluid mixture. This term is built on the postulate that mass transfer does not affect the boiling mechanism itself but does affect the driving force.

Likewise, the microscopic heat-transfer term takes accepted empirical correlations for pure-component pool boiling and adds corrections for mass-transfer and convection effects on the driving forces present in pool boiling. In addition to dependence on the usual physical properties, the extent of superheat, the saturation pressure change related to the superheat, and a suppression factor relating mixture behavior to equivalent pure-component heat-transfer coefficients are correlating functions.

2. Description of Gas–Vapor Systems

In engineering applications, the transport processes involving heat and mass transfer usually occur in process equipment involving vapor–gas mixtures where the vapor undergoes a phase transformation, such as condensation to or evaporation from a liquid phase. In the simplest case, the liquid phase is pure, consisting of the vapor component alone.

The system of primary interest, then, is that of a condensable vapor moving between a liquid phase, usually pure, and a vapor phase in which other components are present. Some of the gas-phase components may be noncondensable. A simple example would be water vapor moving through air to condense on a cold surface. Here the condensed phase, characterized by T and P, exists pure. The vapor-phase description requires y, the mole fraction, as well as T and P. The nomenclature used in the description of vapor-inert gas systems is given in Table 1.

The humidity term and such derivatives as relative humidity and molal humid volume were developed for the air–water system. Use is generally restricted to that system. These terms have also been used for other vapor–noncondensable gas phases.

For the air–water system, the humidity is easily measured by using a wet-bulb thermometer. Air passing the wet wick surrounding the thermometer bulb causes evaporation of moisture from the wick. The balance between heat transfer to the wick and energy required by the latent heat of the mass transfer from the wick gives, at steady state,

$$-k_Y \cdot A \cdot (Y_1 - Y_w) \cdot \lambda_w = \left(h_g + h_r\right) \cdot A \cdot (T_1 - T_w) \qquad (14)$$

$$T_1 - T_w = \frac{k_Y \lambda_w}{\left(h_g + h_r\right)} (Y_w - Y_1) \qquad (15)$$

If radiant energy transfer can be prevented, the following equation is used:

$$T_1 - T_w = \frac{k_Y \cdot \lambda_w}{h_g} (Y_w - Y_1) \qquad (16)$$

Thus, a measurement of the wet-bulb temperature, T_{w}, and the temperature T_1, allows the molal humidity, Y_1, to be calculated because Y_{w} is known. The use of molal humidity as the mass-transfer driving force is conventional and convenient because of the development of humidity data for, especially, the air–water system. The mass-transfer coefficient must be expressed in consistent units.

Another relationship between temperature and humidity results from considering the path of T and Y during an adiabatic saturation process. If a countercurrent packed column exists such that no heat flows from

Table 1. Definitions of Humidity Terms

Term33	Meaning	Units	Symbol[a]
humidity	vapor content of a gas	mass vapor per mass noncon-densable gas	$Y' = Y\frac{M_a}{M_b}$
molal humidity	vapor content of a gas	moles vapor per mole noncon-densable gas	Y
relative saturation or relative humidity	ratio of partial pressure of vapor to partial pressure of vapor at saturation	kPa/kPa, or mole fraction per mole fraction, expres-sed as %	$\frac{y}{y_s} \times 100$
percent saturation or percent humidity	ratio of concentration of vapor to the concen-tration of vapor at saturation with concentrations expressed as mole ratios	mole ratio per mole ratio, expressed as %	$\frac{Y}{Y_s} \times 100$
molal humid volume	volume of 1 mol of dry gas plus its associated vapor	m^3/mol[a,b]	$V_h = (1 + Y) \times 0.0224\frac{T}{273} \times 1.013\ P^{-1}$
molal humid heat	heat required to raise the temperature of 1 mol of dry gas plus its associated vapor 1°C	J/(mol·°C)[a]	$c_h = c_b + Y_{c_a}$
adiabatic saturation temperature	temperature that would be attained if the gas were saturated in an adiabatic process	°C or K	T_{sa}
wet-bulb temperature	steady-state temperature attained by a wet-bulb thermometer under standardized conditions	°C or K	T_{w}
dew-point temperature	temperature at which vapor begins to condense when the gas phase is cooled at constant pressure	°C or K	T_{d}

[a]Concentration is on the basis of dry gas.
[b]When T is in K and P is in Pa.

or to the surroundings and the liquids (water) stream is recycled, the gas stream (air) passes once through the unit. In this case the liquid reaches a steady-state temperature. If the column is very tall, the gas exit temperature would reach the temperature of the recycled liquid. Figure 1 shows the physical arrangement and the nomenclature. Material and energy balances written for an envelope encircling the exit and entrance streams from this column using enthalpies in terms of molal humid heats, latent heats, and liquid heat capacities yield the following:

$$C_{h_1} \cdot (T_{\text{sa}} - T_1) = \lambda_{\text{sa}} \cdot (Y_1 - Y_{\text{sa}}) \qquad (17)$$

where sa refers to the adiabatic saturation condition and point 1 is any initial condition. This is the adiabatic saturation equation that traces the path of a moist gas stream as it is humidified under adiabatic conditions.

For the air–water system, Lewis recognized that $C_h = h_g/k_Y$, based on empirical evidence. Thus, the adiabatic saturation equation is identical to the wet-bulb temperature line. In general, again based on empirical evidence (21),

$$\frac{h_g}{k_Y} = C_h\left(\frac{Sc}{Pr}\right)^{0.56} \qquad (18)$$

whereas, normally, $6.83 < h_g/k_Y < 7.82$, for air $ScPr0.70$, and $h_g/k_Y = C_h = 6.94$.

A closer look at the Lewis relation requires an examination of the heat- and mass-transfer mechanisms active in the entire path from the liquid–vapor interface into the bulk of the vapor phase. Such an examination yields the conclusion that, in order for the Lewis relation to hold, eddy diffusivities for heat- and mass-transfer

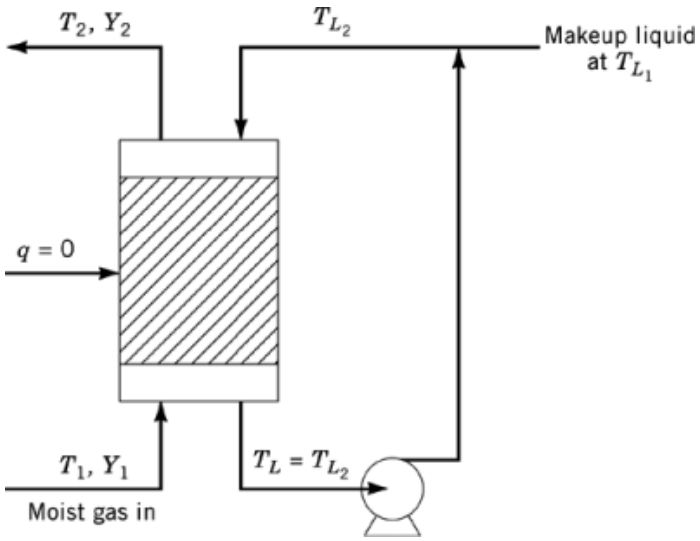

Fig. 1. The adiabatic saturation process, where for a saturation column, $T_2 = T_{sa}$, and $Y_2 = Y_{sa}$.

must be equal, as must the thermal and mass diffusivities themselves. This equality may be expected for simple monatomic and diatomic gases and vapors. Air having small concentrations of water vapor fits these criteria closely.

The thermodynamic properties of a vapor–gas mixture, ie, two components, one of which is condensable, are usually presented on a humidity diagram. Figure 2 is the humidity diagram for the air–water vapor phase at normal atmospheric pressure, where humidity is plotted against temperature. Curves are given for saturated vapor and for constant values of relative humidity. Also plotted are lines of constant wet-bulb temperature, or adiabatic saturation lines. These are nearly straight lines having negative slopes slightly less than 30°. These lines are also lines of nearly constant enthalpy, as can be seen by rearranging equation 17. The deviation is in the variations of humidity heat and latent heat along the path. The chart shows values of the enthalpy at saturation as well as lines of constant enthalpy deviation. Thus, the enthalpy can be found by adding the enthalpy deviation to the enthalpy of the saturated gas phase at the wet-bulb temperature. A copy of this diagram covering a greater temperature span is available (see Drying).

Figure 3 is the humidity chart diagram in molar quantities where enthalpy deviations are not given. Enthalpy may also be calculated from the enthalpy of saturated air and of dry air using % saturation:

$$H = H_{\text{dry}} + \left(H_{\text{sat}} - H_{\text{dry}}\right) \cdot (\%\ \text{saturation}) \qquad (19)$$

Figure 3 gives the % humidity as the measure of vapor concentration, whereas Figure 2 gives relative humidity in %.

For systems other than air–water vapor or for total system pressures different from 101.3 kPa (1 atm), humidity diagrams can be constructed if basic phase-equilibria data are available. The simplest of these relations is Raoult's law, applicable at small solute concentrations:

$$P \cdot y_s = p_i^{\circ} \cdot x_i \qquad (20)$$

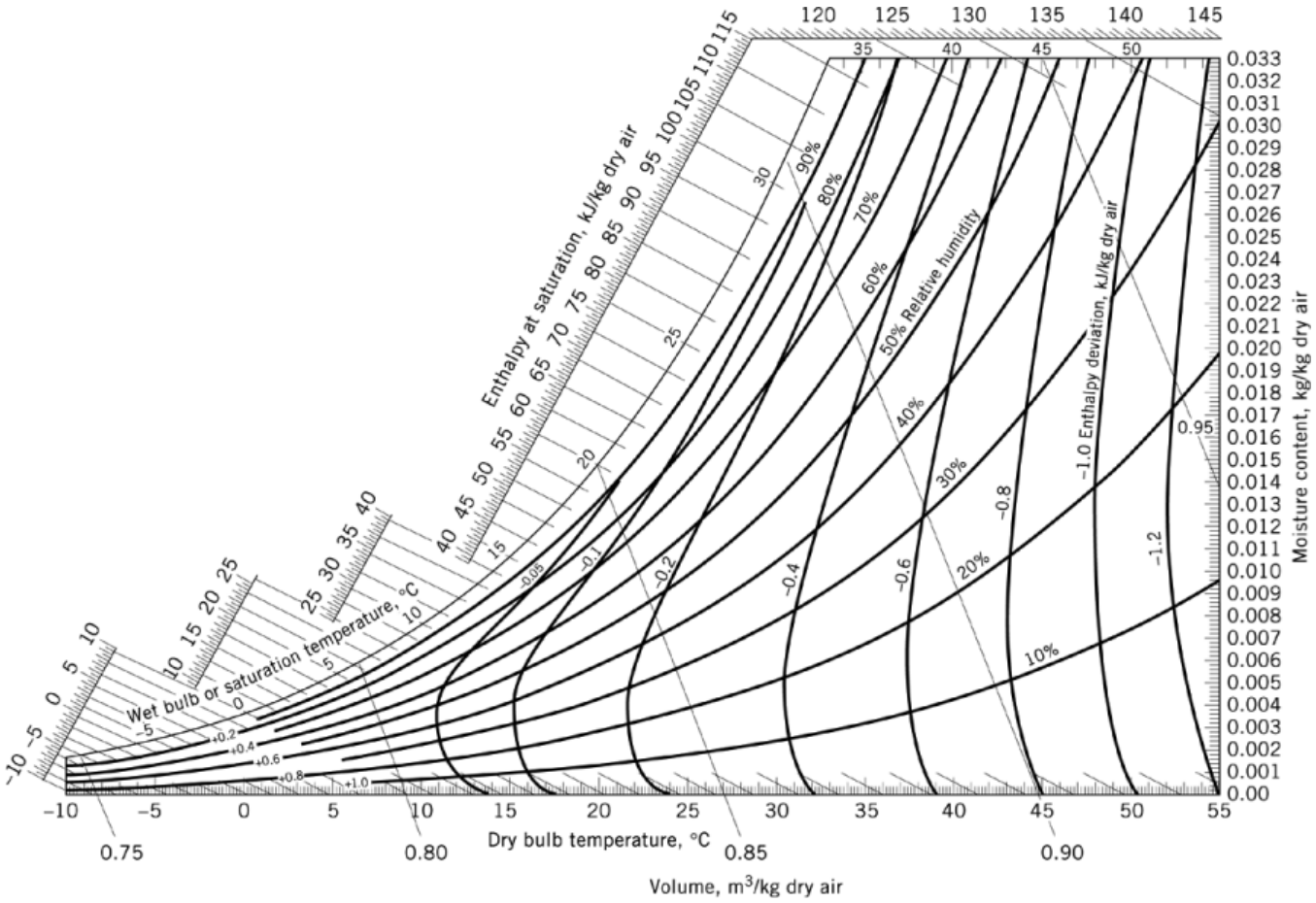

Fig. 2. Psychrometric chart. Below 0°C properties and enthalpy deviation lines are for ice. Courtesy of Carrier Corp. To convert kJ to kcal, divide by 4.184.

For a two-component system in which one component exists only in the vapor phase, equation 20 is reduced to the following:

$$y_s = \frac{H_s}{1 + H_s} = \frac{p_i^\circ}{P} \qquad (21)$$

3. Calculations for Humidification and Dehumidification Processes

Figure 4 shows the general arrangement and nomenclature for a humidification or dehumidification process, where the subscript 1 refers to the bottom of the column, and subscript 2 to the top. Steady state is assumed. Flow rates and compositions are given in molar terms because this simplifies the results.

Total material, condensable component, and energy balances can be written for the entire column:

$$L_1 - L_2 = V_1 - V_2 \qquad (22)$$

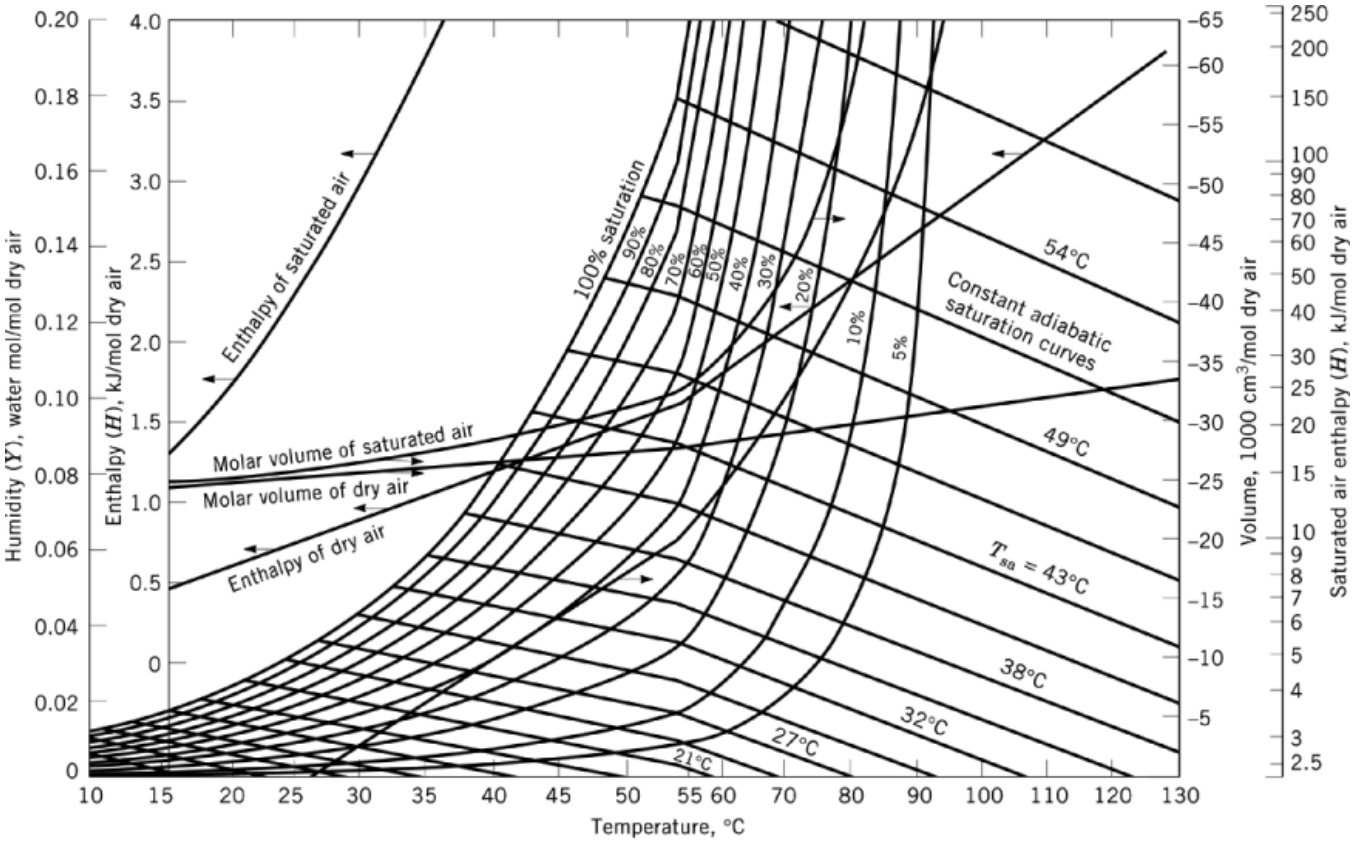

Fig. 3. Humidity chart for the air–water system, molal quantities. To convert kJ to Btu, divide by 1.054; to convert cm^3 to ft^3, multiply by 35.31×10^{-6}.

$$V'\cdot(Y_2 - Y_1) = L_2 - L_1 \qquad (23)$$

$$L_2\cdot H_{L_2} + V'\cdot H_{V_1} + q = L_1\cdot H_{L_1} + V'\cdot H_{V_2} \qquad (24)$$

Generally, q is small because the outside area is not large in comparison to the amount of heat being transferred, and the energy balance can be simplified. In these conditions it is also convenient to write balances over a differential section of the column. These balances yield the following:

$$V'\cdot dY = dL \qquad (25)$$

$$V'\cdot dH_V = d\,(L\cdot H_L) \qquad (26)$$

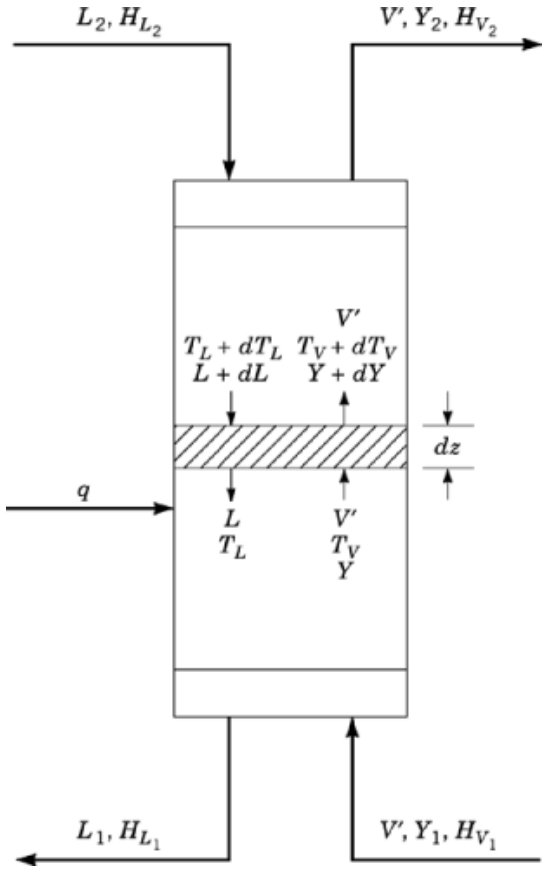

Fig. 4. Arrangement and nomenclature for general humidification–dehumidification process.

If the amount of evaporation is small, the change in enthalpy in the liquid phase can be taken as a result of temperature change alone. Using an average (av) liquid flow rate, the following is derived:

$$V' \cdot dH = L_{\text{av(g)}} \cdot C_L \cdot dT_L \qquad (27)$$

Similarly, the vapor enthalpy can be expressed in terms of humid heat and latent heat in relation to a base condition:

$$V' \cdot dH = V' \cdot d\left[C_h \cdot (T_V - T_o) + Y \cdot \lambda_o\right] = V' \cdot C_h \cdot dT_V + V' \cdot \lambda_o \cdot dY \qquad (28)$$

The energy transferred on both sides of the interface in equation 28 can also be written in terms of the appropriate rate expressions. For the liquid phase, it is

$$\frac{L_{\text{av(g)}}}{S} C_L \cdot dT_L = h_L \cdot a \left(T_L - T_i\right) \cdot dz \qquad (29)$$

For the gas phase, energy transfers both as a result of a thermal driving force and as a by-product of vaporization. Thus,

$$\frac{V'}{S} C_h \cdot dT_V = h_g \cdot a \,(T_i - T_V) \cdot dz \qquad (30)$$

and

$$\frac{V'}{S} \lambda_o \cdot dY = \lambda_o \cdot k_Y \cdot a \,(Y_i - Y) \cdot dz \qquad (31)$$

Combining these two mechanisms for gas-phase transfer, as done in equation 28, yields

$$\frac{V'}{S} dH_V = h_g \cdot a \,(T_i - T_V) \cdot dz + \lambda_o \cdot k_Y \cdot a \,(Y_i - Y) \cdot dz \qquad (32)$$

Rearranging equation 32 and defining the ratio $h_c \cdot a/(k_Y \cdot a \cdot C_h)$ as r, the psychrometric ratio, give

$$\frac{V'}{S} dH_V = k_Y \cdot a \,[(C_h \cdot r \cdot T_i + \lambda_o \cdot Y_i) - (C_h \cdot r T_V + \lambda_o \cdot Y)] \cdot dz \qquad (33)$$

For the air–water system, the Lewis relation shows that $r = 1$. Under these conditions, the two parenthetical terms on the right-hand side of equation 33 are enthalpies, and equation 33 becomes the design equation for humidification operations:

$$\frac{V'}{S} dH_V = k_Y \cdot a \,(H_i - H_V) \cdot dz \qquad (34)$$

or

$$\int_{H_{V_1}}^{H_{V_2}} \frac{V' \cdot dH_V}{k_Y \cdot a S (H_i - H_V)} = \int_0^z dz = z \qquad (35)$$

The simplification of equation 33 to equation 34 is possible only if $r = 1$; that is, for simple monoatomic and diatomic gases. For other systems the design equation can be obtained by a direct rearrangement of equation 33.

Although equation 35 is a simple expression, it tends to be confusing. In this equation the enthalpy difference appears as driving force in a mass-transfer expression. Enthalpy is not a potential, but rather an extensive thermodynamic function. In equation 35, it is used as enthalpy per mole and is a kind of shorthand for a combination of temperature and mass concentration terms.

The integration of equation 35 requires a knowledge of the mass-transfer coefficient, $k_Y \cdot a$, and also of the interface conditions from which H_i could be obtained. Combining equations 27, 28, and 34 gives a relation balancing transfer rate on both sides of the interface:

$$\frac{V'}{S} dH_V = h_L \cdot (T_L - T_i) \cdot dz = k_Y \cdot a \,(H_i - H_V) \cdot dz \qquad (36)$$

or

$$\frac{-h_L \cdot a}{k_Y \cdot a} = \frac{H_V - H_i}{T_L - T_i} \qquad (37)$$

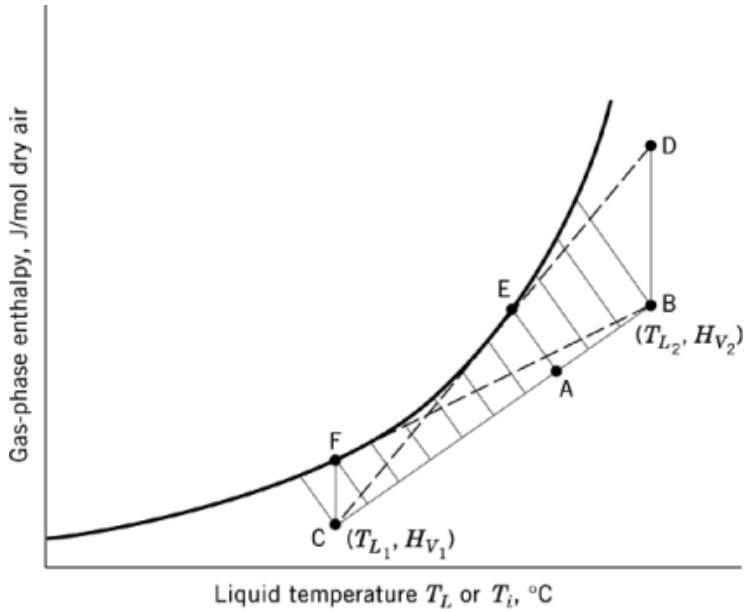

Fig. 5. Adiabatic gas–liquid contacting, graphical representation where point A is an arbitrary point along the column; line CAB is the operating line having slope of $L_{av(g)} \cdot C_L / V'$; point E represents the interface conditions corresponding to point A; and the tie line AE has slope of $h_L \cdot a / (k_Y \cdot a)$. The bold line defines the equilibrium curve, H_i vs T_i. Conditions shown are those of a water-cooling process. To convert J to Btu, divide by 1054.

Thus, the enthalpy and temperature of the vapor–liquid interface are related to the liquid temperature and gas enthalpy at any point in the column through a ratio of heat- and mass-transfer coefficients.

The integration can be carried out graphically or numerically using a computer. For illustrative purposes the graphical procedure is shown in Figure 5. In this plot of vapor enthalpy (H_V or H_i) vs liquid temperature (T_L or T_i), the curved line is the equilibrium curve for the system. For the air–water system, it is the 100% saturation line taken directly from the humidity diagram (see Fig. 3).

The locus of corresponding T_L and H_V points, the operating line for the column, can be obtained by assuming that V' and $L_{av(g)}$ change little and by integrating equation 27 along the length of the column.

$$\int_{H_{v_1}}^{H_{v_2}} V' \cdot dH = \int_{T_{L_1}}^{T_{L_2}} L_{avg(g)} \cdot C_L \cdot dT \qquad (38)$$

$$V' \cdot \left(H_{V_2} - H_{V_1}\right) = L_{av(g)} \cdot C_L \cdot \left(T_{L_2} - T_{L_1}\right) \qquad (39)$$

or

$$\frac{H_{V_2} - H_{V_1}}{T_{L_2} - T_{L_1}} = \frac{L_{av(g)} \cdot C_L V'}{V'} \qquad (40)$$

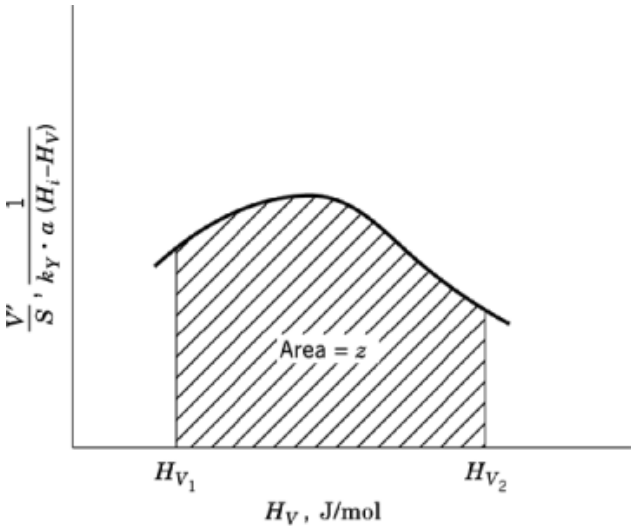

Fig. 6. Integration of the design equation (eq. 35).

Thus, the locus is a straight line, assuming that the ratio on the right side of equation 40 is constant. The actual location of the line can be obtained if both end points are known or if one end point and the slope $(L_{\mathrm{av(g)}} \cdot C_L / V')$ can be determined.

In Figure 5 the locus of interface points passes through points F and E. The operating line goes from B to C. In addition to specifying two points on the line itself, B and C, or the slope and one of these points, the column could be required to operate at some convenient gas flow rate greater than minimum. Here the minimum gas flow rate required to cool the liquid from 60 to 30°C is given by line CD. Another possible limiting condition would be the flow of gas with the largest wet-bulb temperature possible to allow water to cool from 60 to 30°C, no matter how large the column (line BF). A design and operating condition can be determined as an acceptable approach to either of these.

Once the operating line is set, interface conditions corresponding to any point on the operating line can be found if heat- and mass-transfer coefficients are available. Then a line of slope $-h_L \cdot a/(k_Y \cdot a)$ connects a point on the operating line, eg, point A, with its corresponding interface condition, point E. This information allows the integration of equation 35 to give the column height. The method is shown graphically in Figure 6, although again a numerical solution is possible.

3.1. Determination of the Gas-Phase Temperature

The development given above is in terms of interface conditions, bulk liquid temperature, and bulk gas enthalpy. Often the temperature of the vapor phase is important to the designer, either as one of the variables specified or as an important indicator of fogging conditions in the column. Such a condition would occur if the gas temperature equaled the saturation temperature, that is, the interface temperature. When fogging does occur, the column can no longer be expected to operate according to the relations presented herein but is basically out of control.

Gas-phase temperatures have been obtained by an extension of the graphical method illustrated (22). When equation 30 is divided by equation 34, the result is

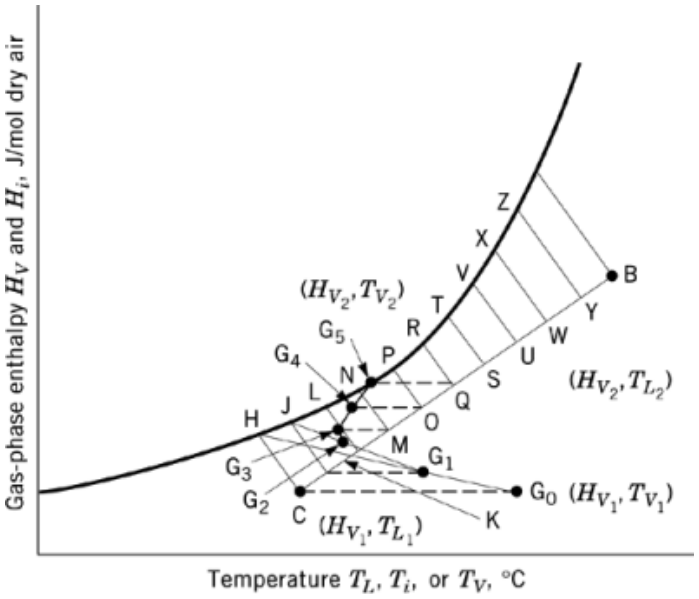

Fig. 7. Determination of the bulk gas-phase temperature path.

$$\frac{V' \cdot C_h \cdot dT_V}{V' \cdot dH_V} = \frac{h_g \cdot a \cdot (T_i - T_V) \cdot dz}{k_Y \cdot a \cdot (H_i - H_V) \cdot dz} \qquad (41)$$

or

$$\frac{dT_V}{dH_V} = \frac{h_g \cdot a}{C_h \cdot k_Y \cdot a} \cdot \frac{(T_i - T_V)}{(H_i - H_V)} = \frac{T_i - T_V}{H_i - H_V} \qquad (42)$$

The last expression of equation 42 is obtained by applying the Lewis relation, $C_h = h_c/k_Y$. If the differentials of equation 42 are replaced by finite differences, the following obtains:

$$\frac{\Delta T_V}{\Delta H_V} \approx \frac{T_i - T_V}{H_i - H_V} \qquad (43)$$

In effect, equation 43 states that the temperature and enthalpy values of the bulk gas phase continuously approach the interface condition at the same point in the column as that for which the gas-phase conditions apply. The graphical application is illustrated in Figure 7. The gas-phase temperature and enthalpy at the bottom of the column are usually known and are plotted at point G_0. The interface conditions at the bottom of the column are given at point H. Then by equation 43 the line GH is the path followed by the gas-phase temperature. This path is followed until the interface condition shifts noticeably, perhaps to point J corresponding to a bulk liquid temperature at point I. Then the gas temperature line approaches point J. The interface conditions shift toward point Z, continuously changing the direction of the gas temperature line. The points at which the line changes slope depend on the intervals chosen along the operating line. Here G_1 corresponds to point I, G_2 to point K, G_3 to point M, G_4 to point O, etc.

In the example developed herein fogging occurs at about the time the gas reaches the top of the column. That is far from inevitable and would not have occurred if the operating line had terminated at point U.

The method thus outlined allows the development of a conceptual understanding of the limits of operation of a humidification column. For actual design, the simplifications used herein may be avoided by handling the fundamental equations numerically by computer.

3.2. Transfer Coefficient

The design method described depends for its utility on the availability of mass- and heat-transfer coefficients. Typically, $k_Y \cdot a$ and $h_L \cdot a$ are needed. These must be obtained from the standard correlations for mass and heat transfer, from data reported in the literature (23–30), or from data presented by equipment makers for particular packing (31–33). When this type of information is not available, it is possible to determine heat- and mass-transfer coefficients by a single test using the packing material of interest in a pilot-sized tower. If a steady state is obtained, measurement of air- and water-inlet and -outlet temperatures, and air-inlet and -outlet wet- and dry-bulb temperatures comprises all the necessary information. Interface and operating lines on a T_L–H_V diagram, such as Figure 5, are directly obtained. Because column heights are known, the value of $h_L \cdot a/(k_Y \cdot a)$ can be obtained by trial and error with the integration demonstrated in Figure 6 and adjustment of the slope of the operating interface condition line until z_{calc} equals the actual column height.

3.3. Overall Coefficients

Often overall coefficients of heat and mass transfer are available, rather than the film coefficients used earlier. In that case equation 35 can be rewritten as

$$\int_{H_{V_1}}^{H_{V_2}} \frac{V' \cdot dH_V}{k_Y \cdot a \cdot S \cdot (H^* - H_V)} = \int_0^z dz = z \qquad (44)$$

If $k_Y \cdot a$ is constant, this can be written as

$$\frac{V'}{k_Y \cdot a \cdot S} \int_{H_{V_1}}^{H_{V_2}} \frac{dH_V}{(H^* - H_V)} = \text{HTU}\cdot\text{NTU} = z \qquad (45)$$

4. Humidification and Dehumidification Equipment

The addition or removal of a condensable component to or from a noncondensable gas can be accomplished by direct contact between the vapor and the gas. This may be done in a countercurrent tower, usually packed as described elsewhere (see Adsorption; Distillation). The direction of transfer depends on the temperatures of the two streams. Such operations can also be done using spray ponds in which a grid of nozzles sprays liquid, usually water, into the gas phase, usually air. If the air is relatively dry, liquid evaporates into it, both humidifying the air and cooling the liquid. If a large surface of water is available, the same process may be carried out through evaporation from the surface of lake or pond. Usually the purpose is the cooling of process water. As hot water is discharged into the pond, the surface temperature of the pond rises until evaporation (qv) balances the incoming thermal load. A large enough pond surface must be supplied to allow evaporation to balance the thermal load at a manageable temperature rise. This area requirement may exceed the availability of land in the plant site region.

Humidification processes also occur in spray contactors often used to scrub minor components from a gas stream. Here the gas passes through successive sprays of liquid. The liquid is often water but may be specially compounded to enhance absorption of the component to be removed.

4.1. Water-Cooling Towers

By far the most common and large-scale mode of humidification processing is in water-cooling towers. As supplies of cooling water become more strained, and as discharge water temperatures are more closely controlled, water cooling and recirculation rather than once-through water use become more common. Two general types of direct-contact cooling towers are in use. The forced-draft tower depends on fans to move the air through the tower. Typically, the tower consists of a set of louvres and baffles over which the water falls, breaking into films and droplets. Air flow may be across this cascading liquid or countercurrent of it. Often both flow arrangements exist in the same tower. Figure 8 shows a cross-sectional view of a cooling tower. Here air flows across the cascading liquid, drawn by a fan located in the outlet duct. In other arrangements the fan can be placed to push the air through the tower.

There are several internal gridwork arrangements, all designed to enhance splashing and film formation in order to give a large water–air interface and allow a low pressure drop in the air stream passing through. The lattice members were traditionally wood-treated to prevent biological and corrosion attack. More recently, different materials such as transite, various plastic laminates, and ceramics have been used. Packing design has also become more and more specialized, and proprietary designs are offered by most cooling-tower makers.

The thermal design of cooling towers follows the same general procedures already presented. Integration of equation 35 is usually done numerically using the appropriate software, mass-transfer coefficients, saturation enthalpies, etc. In mechanical-draft towers the air and water flows are both supplied by machines, and hence flow rates are fixed. Under these conditions the design procedure is straightforward.

4.2. Natural-Draft Cooling Towers

In a natural-draft cooling tower (Fig. 9) the driving force for the air is provided by the buoyancy of the air column in a very tall stack. Stack heights of 100 m are common, and as power-plant sizes increase, the size of single towers is likely to increase also. In the absence of a fan, the air flow rate, G, is no longer an independent variable, but is dependent on the design and operating conditions of the tower. The governing equation for air flow becomes

$$z_t \cdot \Delta\rho = N \frac{G^2}{\rho g_c}$$

where $\Delta\rho$ is the average density difference between the outside air and the air in the stack; z_t is the height of the tower, and N, the resistance to air flow through the tower in velocity heads, is specific for a given tower and can usually be expressed as a constant (34).

For a natural-draft tower, equations 46 and 44 must be solved simultaneously, introducing an expression for $\Delta\rho$ as a function of conditions inside and outside the tower. Up until 1955, this was a cumbersome procedure, and a number of approximate methods were devised to simplify the calculation. Since then, the whole calculation has been done using computer software. For a tower of given dimensions, the air flow can be guessed and the thermal performance and pressure loss calculated. From the thermal performance, the density difference, $\Delta\rho$, can be calculated and the left side of equation 46 compared to the other side. When the correct air flow has been guessed, the equation is satisfied. Iterative procedures using rapid convergence can easily be devised (see Computer-aided design and manufacturing (CAD/CAM); Computer-aided engineering (CAE)) (35). Cooling-tower manufacturers express confidence in their ability to design cooling towers that meet guaranteed performance and to predict off-design behavior.

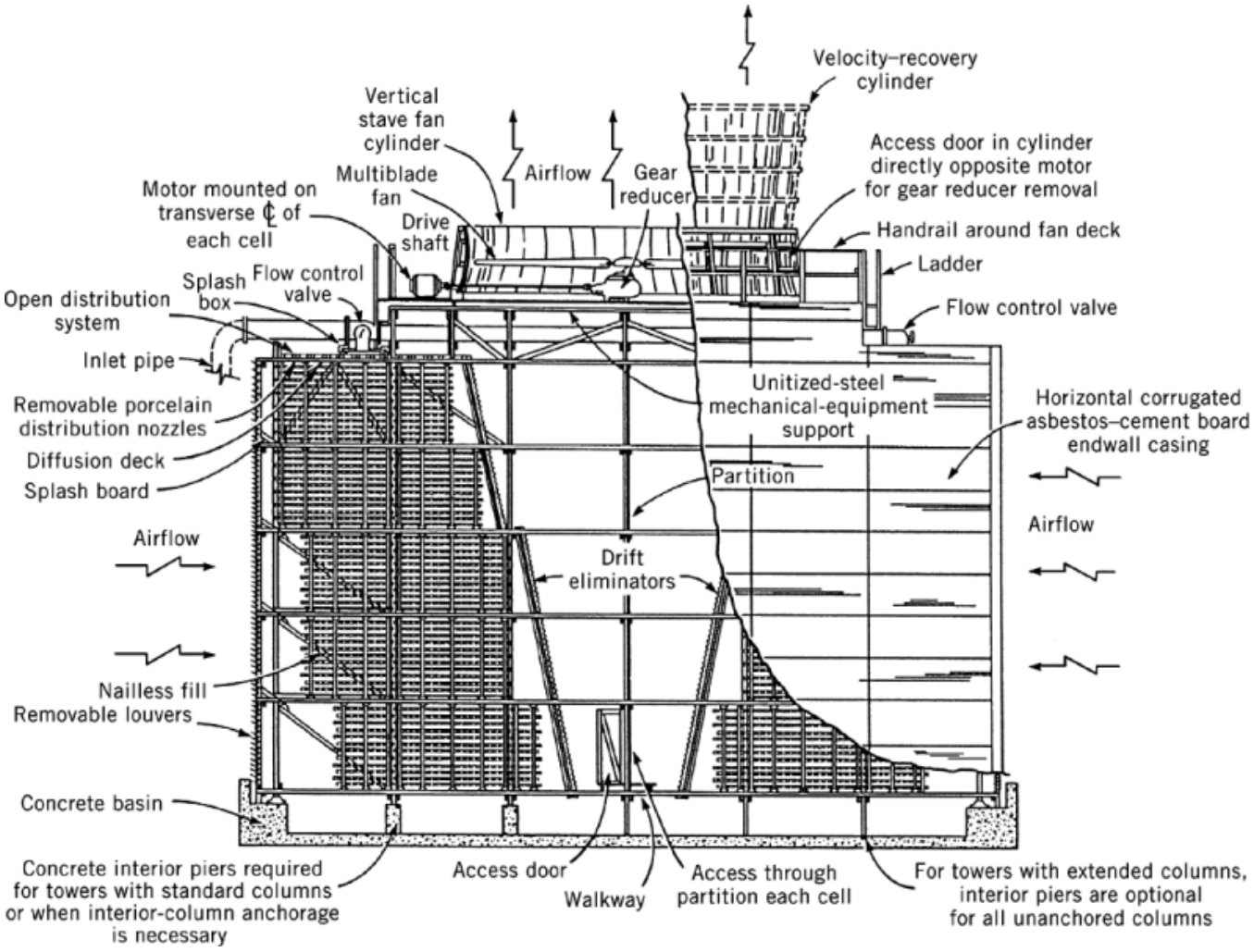

Fig. 8. Transverse cross-sectional view of double-flow induced-draft cooling tower. Courtesy of The Marley Co.

4.3. Approximate Methods for Predicting Natural-Draft Cooling-Tower Performance

Approximate methods, no longer needed for design work, are useful for rapid estimates of the effects of changing conditions on performance. In addition, a good grasp of the approximate theories leads to a better physical understanding of tower behavior.

An approximate method for integrating equation 44, ie, Merkel's approximation (34, 36), leads to the following:

$$\frac{H_m^* - H_2}{T_{L_1} - T_{L_2}} = \frac{L}{2G} + \frac{L}{Kaz} \qquad (47)$$

Using Merkel's approximation and knowing the desired thermal performance, the flow rates, and transfer coefficient, z, can quickly be calculated. The difficulty with this method is that errors of $\geq$10% in z can arise if the cooling range $T_1 - T_2$ is larger than a few degrees.

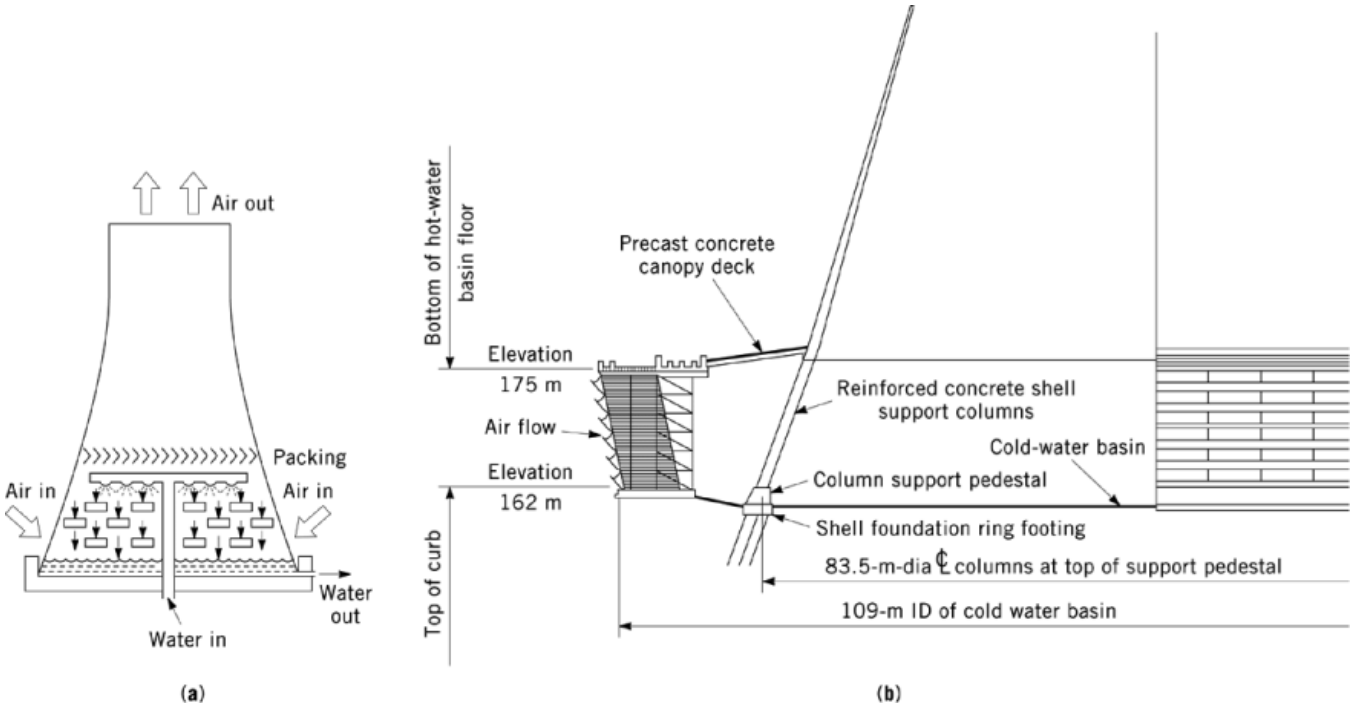

Fig. 9. Natural-draft cooling tower: (**a**) general tower drawing for countercurrent air–water flow arrangement; (**b**) sectional drawing showing arrangement for cross flow of air–water.

Equations 46 and 47 have been combined to obtain rapid approximate methods for predicting cooling tower performance (34, 37). The most interesting result is obtained from a rather simple analysis (38). If A is the cross-sectional area of the packing, then the liquid total flow rate $W_L = AL$, and the air flow rate $W_G = AG$. Substituting for G in equation 46 gives, with some rearrangement, the following:

$$\frac{A(z_t)^{1/2}}{(N/2)^{1/2}} = \frac{W_G}{(\Delta\rho)^{1/2}(\rho)^{1/2}} \qquad (48)$$

Equation 48 equals D, the duty coefficient of the tower. Let $(N/2)^{1/2} = C^{3/2}$, then

$$\frac{A(z_t)^{1/2}}{C^{3/2}} = -\frac{W_G}{(\Delta\rho)^{1/2} \cdot (\rho)^{1/2}} = D \qquad (49)$$

Reference 34 shows that

$$\Delta\rho = 13.465 \times 10^{-5}\,(\Delta T_V + 0.3124\Delta H) \qquad (50)$$

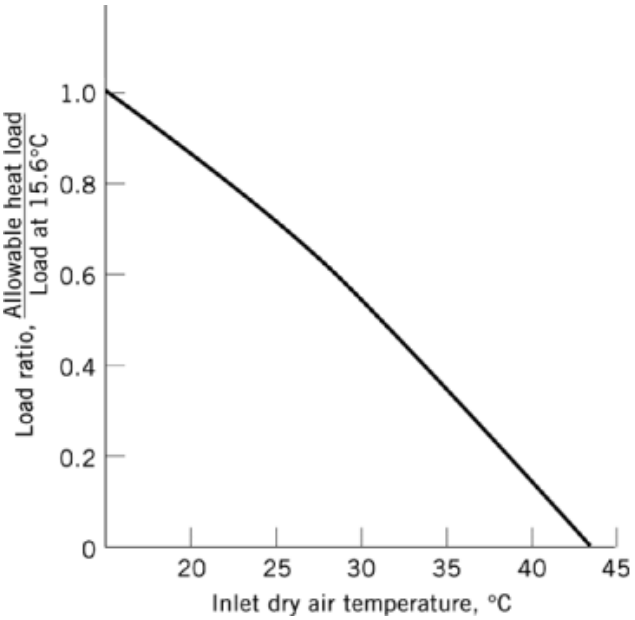

Fig. 10. Effect of inlet dry air temperature on allowable load, where the inlet relative humidity is 50%; water-inlet temperature is 43.3°C; water exit temperature is 32.2°C.

Rearranging equation 50, applying the energy balance, and assuming air at standard conditions enters the tower yield (38):

$$\frac{W_L}{D} = 90.59\,\frac{\Delta H}{\Delta T}\,(\Delta T + 0.3124\Delta H)^{1/2} \qquad (51)$$

For most cooling towers in the United Kingdom, the exit air is saturated at a temperature close to the mean water temperature in the tower. Hence, if the water temperatures and the air inlet conditions are known, ΔH, ΔT_{L}, and ΔT_{V} can all be calculated, and W_{L}/T can be determined. It was found that the quantity C was approximately constant for these towers, ca 0.4–0.5 (34). If the value of C is known for a given tower, then the left side of equation 49 can be computed and, setting this equal to D, the allowable liquid flow rate can be found. Alternatively, when W_{L}, T_{L1}, and air-inlet conditions are given, the equations can be used to find T_{L2}. A rapid estimate of the effects of off-design conditions can thus be made. Reference 38 presents a nomogram of these equations to facilitate the calculation (see Engineering, chemical data correlation).

Natural-draft cooling towers are extremely sensitive to air-inlet conditions owing to the effects on draft. It can rapidly be established from these approximate equations that as the air-inlet temperature approaches the water-inlet temperature, the allowable heat load decreases rapidly. For this reason, natural-draft towers are unsuitable in many regions of the United States. Figure 10 shows the effect of air-inlet temperature on the allowable heat load of a natural-draft tower for some arbitrary numerical values and inlet rh of 50%. The trend is typical.

4.4. Trends in Cooling-Tower Use and Development

Natural-draft cooling towers had been rare in the United States because ample water supplies were available for power-plant cooling, and natural-draft towers are best suited for large heat loads. Mechanical-draft towers

were used in large numbers for industrial applications and occasionally for power plants. A dramatic change in this situation has occurred. Almost all large post-1980 power plants require cooling towers. Limitations on cooling water use and the return of warm water to rivers has forced the use of all cooling towers. Towers allow the heat load to be dissipated to the air rather than into natural water. The treating of recycled cooling water may pose hazards to aquatic animals, crops, etc, near the tower. In the southern United States, mechanical-draft towers dominate the field; in the northern United States, the situation is not as clear. Because of earlier over-building and public attitudes toward cost recovery, few power plants were built in the 1980s or early 1990s. Many existing plants were, however, upgraded. The issues involved in a decision have been discussed (39, 40).

The initial cost of a mechanical-draft cooling tower for a power plant is relatively low, ca $10.00/kW more than a direct-stream cooling system. However, the power required to run the fan is significant, and maintenance must also be considered. In a large power plant, many mechanical-draft towers are required, covering a large area of ground, and problems of water and power distribution become acute. In addition, the plume is discharged close to the ground and can be a source of fog.

The final cost of a natural-draft tower is substantially higher, ca $20.00/kW. However, the maintenance costs are much lower because there are no fans or electrical drives. The natural-draft tower occupies less ground space than the corresponding group of mechanical-draft towers. Additionally, because the plume is discharged $\geq$100 m from the ground, it is much less likely to cause local ground fog. Thus the natural-draft tower is frequently more attractive, and may be chosen even if there is a slight overall cost disadvantage.

The economics of cooling towers has been discussed (38, 41). A worthwhile evaluation of the optimum configuration must take into account the interaction between tower performance and plant performance. For example, in considering the additional expense of a cooling tower vs a direct-stream cooling system, it is desirable to optimize the whole plant for each system rather than add the cooling tower to a system optimized for run-of-the-river cooling. Consequently, it is not possible to produce general-cost curves for cooling towers. Each installation must be evaluated separately.

As of the mid-1990s, a large natural-draft cooling tower could cost approximately $12,000,000, according to general cost analysis calculations and annual construction cost ratios. That cost was divided almost equally between the foundation, the packing and water-distribution system, and the shell. Therefore, large cost reductions in any of these items can have a significant effect. Newer, light packings are being developed in a variety of materials, leading to some cost improvements. Packings may be built of fiber-reinforced polymers, chosen for resistance to the heated water to which they are to be exposed, as well as for strength, weight, and cost considerations. The tower shell, made of reinforced concrete, has a hyperbolic shape chosen mainly for structural rather than aerodynamic reasons. A hyperbolic shell requires less concrete than an equally strong cylindrical shell. It seems unlikely that important cost reductions in the shell or foundation can be made.

When all the expenses involved in using wet cooling towers on a power plant are considered, it appears that a mechanical-draft cooling tower system may raise the cost of generating electricity by ca 3%, and a natural-draft tower by ca 6%, over the generating cost of a direct river-cooled power plant. These figures are approximate, but show the effects of a thermal pollution regulatory program on the cost of generating electricity (see Thermal pollution).

4.5. Cooling-Tower Plumes

An important consideration in the acceptability of either a mechanical-draft or a natural-draft tower cooling system is the effect on the environment. The plume emitted by a cooling tower is seen by the surrounding community and can lead to trouble if it is a source of severe ground fog under some atmospheric conditions. The natural-draft tower is much less likely to produce fogging than is the mechanical-draft tower. Nonetheless, it is desirable to devise techniques for predicting plume trajectory and attenuation.

Not only may the cooling-tower plume be a source of fog, which in some weather conditions can ice roadways, but the plume also carries salts from the cooling water itself. These salts may come from salinity in the water, or may be added by the cooling-tower operator to prevent corrosion and biological attack in the column.

Efforts to combat bacteria and corrosion in cooling towers have gone through a long development and are both complex and specific to different waters. Cathodic and anodic inhibitors are used as well as biocides. Systems may include chromates, nitrites, orthophosphates, and ferrocyanides as cathodic inhibitors; zinc, nickel, lead, tin, copper, and silicates as anodic inhibitors; and possibly added materials as biocides and pH controllers. These chemicals can also be carried onto fields surrounding the cooling tower, seriously affecting crop yield or ornamental plantings (see Water, industrial water treatment).

Much work has been done on the modeling of wet cooling-tower plumes; the ultimate aim was to determine their effect on the environment (42–44). The basic approach involves writing the equations of continuity, conservation of energy and momentum, and the equations of motion for the conditions of the plume. These are then solved simultaneously using iterative and numerical methods on large computers. The accuracy of the results depends on whether the boundary conditions and simplifying assumptions are realistic. These are difficult to accomplish because conditions change rapidly, ground configurations are seldom simple, and plume behavior is influenced by a host of casual, nonrepeated situations such as the passing of an airplane or the presence of cloud cover. Modeling owes much to meteorology and especially to the theory of cumulus clouds (see Atmospheric modeling).

The recirculation of cooling water via a cooling tower ultimately removes process heat by evaporating water rather than by warming it, as would be the case with once-through systems. When water is especially scarce, it may be necessary to cool process water by transferring the heat to air through indirect heat transfer. This requires dry cooling towers, which have been built in a few dry regions of the United States. These usually take the form of natural-draft cooling towers in which high surface heat-exchange areas replace the usual gridwork. The air-to-circulating-water heat-transfer process passes heat through a solid surface, thus heat-transfer coefficients are low and enormous heat-transfer areas are required. The cost of such towers may be 10-fold that of wet towers, and the availability of tubing for heat transfer becomes a serious problem.

5. Trends

Work in the area of simultaneous heat and mass transfer has centered on the solution of equations such as 1–18 for cases where the structure and properties of a solid phase must also be considered, as in drying (qv) or adsorption (qv), or where a chemical reaction takes place. Drying simulation (45–47) and drying of foods (48, 49) have been particularly active subjects. In the adsorption area the separation of multicomponent fluid mixtures is influenced by comparative rates of diffusion and by interface temperatures (50, 51). In the area of reactor studies there has been much interest in monolithic and honeycomb catalytic reactions (52, 53) (see Exhaust control, industrial). For these kinds of applications psychrometric charts for systems other than air–water would be useful. The construction of such has been considered (54).

Cooling water is a necessity for temperature control. Most industrially generated heat must be dissipated; water is an obvious receptor because heat transfer is relatively rapid and compact. When the heat load is large it is usually necessary to cool and reuse the water. Thus cooling towers are integral parts of power plants, chemical processing operations, and compression steps, and proper design and operation are critical to the entire process. Relative costs vary widely for different process situations. In power plants, cooling towers might represent 10% of the total capital cost.

Simultaneous heat and mass transfer also occurs in drying processes, chemical reaction steps, evaporation, crystallization, and distillation. In all of these operations transfer rates are usually fixed empirically. The process can be evaluated using either the heat- or mass-transfer equations. However, if the process mechanism

is to be fully understood, both the heat and mass transfer must be described. Where that has been done, improvements in the engineering of the process usually result (see Process energy conservation).

Nomenclature

Symbol	Definition	Units
A	interfacial area	m^2
a	interfacial area per unit column volume	m^{-1}
C	heat capacity	J/(g·K)
D	molecular diffusivity for mass transfer	m^2/h
F	rate of fog formation	mol/h
G	mass flow rate of gas phase	$kg/(h \cdot m^2)$
g_c	force–mass conversion constant	
H	enthalpy	
HTU	height of a transfer unit	
h_c	convective heat-transfer coefficient	
h_r	coefficient for heat transfer by radiative mechanism	
K_a	overall mass-transfer coefficient per volume of contacting column	
k_g	gas-phase mass-transfer coefficient in partial pressure driving force units	
k_L	liquid-phase thermal conductivity	
k_Y	mass-transfer coefficient in gas-phase mole ratio units	
L	liquid stream molar flow rate	
Le	Lewis number	
M	molecular weight	
N	resistance to air flow in velocity heads	
NTU	number of transfer units	
P	total pressure	
Pr	Prandtl number	
p°	vapor pressure	
q	heat flux	
Re	Reynolds number	
r	psychrometric ratio	
S	suppression factor $(\Delta Te/\Delta T)^{0.99}$	
Sc	Schmidt number	
T	temperature	
$\Delta\tilde{T}$	driving force for the binary macroscopic heat transfer	
V	specific volume	
V	gas-phase molar flow rate	
V'	molar flow rate of noncondensable component	
w	total flow rate	mol/time
x	mole fraction in liquid phase	
Y	mole ratio	
Y'	mass ratio	
y	mole fraction in gas phase	
z	height of column	
ϵ	Ackerman correction term, $= m_i \cdot c_{pi} / h_g$	
λ	latent heat of vaporization	
μ	viscosity	
ρ	density	
σ	surface tension	

Nomenclature

Symbol	Definition	Units
Subscripts		
BM	mean value for noncondensing component	
e	effective	
g	gas phase	
h	humid value, including gas and vapor	
i	interface condition	
j	for the jth component (usually less volatile)	
L	liquid phase	
L-only	for the liquid-phase flow alone	
mac	macroscopic contribution	
mic	microscopic contribution	
o	at reference condition	
p	at constant pressure	
s	at saturation	
sa	at adiabatic saturation condition	
V	in the vapor phase	
w	for water, or at wet-bulb temperature	
Y	the mole ratio driving force	
1,2	end points in the process	
2φ	for two-phase flow	
Superscripts		
*	bulk concentration in liquid phase but in gas-phase units, or vice versa	
′	mass rather than mole basis	

BIBLIOGRAPHY

"Simultaneous Heat and Mass Transfer" in *ECT* 3rd ed., Vol. 21, pp. 54–76, by L. A. Wenzel, Lehigh University.

Cited Publications

1. G. Ackerman, *Verh. Dtsch. Ing. Forschungsh.* **382**, 1 (1937).
2. A. P. Colburn and O. A. Hougen, *Ind. Eng. Chem.* **26**, 1178 (1934).
3. A. P. Colburn and T. B. Drew, *Trans. Am. Inst. Chem. Eng.* **33**, 197 (1937).
4. F. Stern and F. Votta, Jr., *AIChE J.* **14**, 928 (1968).
5. D. R. Coughanowr and E. O. Stensholt, *Ind. Eng. Chem. Proc. Des. Dev.* **3**, 369 (1964).
6. J. T. Schrodt, *Ind. Eng. Chem. Proc. Des. Dev.* **11**, 20 (1972).
7. J. T. Schrodt, *AIChE J.* **19**, 753 (1973).
8. R. L. Von Berg, *Recent Advances in Liquid–Liquid Extraction*, Pergamon Press, Oxford, U.K., 1971. X
9. M. M. Dribika and O. C. Sandall, *Chem. Eng. Sci.* **34**, 733 (1979).
10. H. Hikita and K. Ishimi, *Chem. Eng. Com.* **3**, 547 (1979).
11. A. B. M. Abdul Hye, *Simultaneous Heat and Mass Transfer from a Vertical, Isothermal Surface*, Ph.D. dissertation, University of Windsor, Canada, 1979.
12. T. Mizushina, M. Nakajima, and T. Oshima, *Chem. Eng. Sci.* **13**, 7 (1960).
13. J. T. Schrodt and E. R. Gerhard, *Ind. Eng. Chem. Fund.* **7**, 281 (1968).
14. L. W. Florschuetz and A. R. Khan, *Fourth International Heat Transfer Conference*, Paris, France, 1970.
15. O. C. Sandall and M. M. Dribika, *Inst. Chem. Eng. Sym. Ser.* **56**, 2.5/1 (1979).
16. H. J. Barton and O. Trass, *Can. J. Chem. Eng.* **47**, 20 (1969).
17. L. E. Scriven, *Chem. Eng. Sci.* **10**, 1 (1959).

18. F. Marshall and L. L. Moresco, *Int. J. Heat Mass Transfer*, **20**, 1013 (1977).
19. R. A. W. Schock, *Int. J. Heat Mass Transfer*, **20**, 701 (1977).
20. D. L. Bennett and J. C. Chen, *AIChE J.* **26**, 454 (1980).
21. C. H. Bedingfield and T. B. Drew, *Ind. Eng. Chem.* **42**, 1164 (1950).
22. H. S. Mickley, *Chem. Eng. Prog.* **45**, 739 (1949).
23. S. L. Hensel and R. E. Treybal, *Chem. Eng. Prog.* **48**, 362 (1952).
24. J. Lichtenstein, *Trans. ASME*, **65**, 779 (1943).
25. R. L. Pigford and C. Pyle, *Ind. Eng. Chem.* **43**, 1649 (1951).
26. W. M. Simpson and T. K. Sherwood, *Refrig. Eng.* **52**, 535 (1946).
27. A. E. Surosky and B. F. Dodge, *Ind. Eng. Chem.* **42**, 1112 (1950).
28. F. P. West, W. D. Gilbert, and T. Shimizu, *Ind. Eng. Chem.* **44**, 2470 (1952).
29. J. Weisman and E. F. Bonilla, *Ind. Eng. Chem.* **42**, 1099 (1950).
30. F. Yoshida and T. Tanaka, *Ind. Eng. Chem.* **43**, 1467 (1951).
31. *Countercurrent Cooling Tower Performance*, J. F. Prichard Co., Kansas City, Mo., 1957.
32. *Technical Bulletins R-54-P-5, R-58-P-5*, Marley Co., Kansas City, Mo., 1957.
33. *Performance Curves*, Cooling Tower Institute, Houston, Tex., 1967.
34. H. Chilton, *Proc. IEE, Supply Sect.* **99**, 440 (1952).
35. J. R. Singham, *The Thermal Performance of Natural Draft Cooling Towers*, Imperial College of Science and Technology, Department of Mechanical Engineering, London, 1967.
36. H. B. Nottage, *ASHRAE Trans.* **47**, 429 (1941).
37. I. A. Furzer, *Ind. Eng. Chem. Proc. Des. Dev.* **7**, 555 (1968).
38. S. M. Dalton, D. V. Giovanni, J. S. Maulhetsch, G. T. Preston, and K. E. Yeager, in R. A. Meyers, ed., *Handbook of Energy Technology and Economics*, John Wiley and Sons, Inc., New York, 1983.
39. C. Waselkow, *National Conference on Thermal Pollution*, Federal Water Pollution Control Administration and Vanderbilt University, Nashville, Tenn., 1968.
40. W. R. Shade and A. F. Smith, in Ref. 39.
41. B. Berg and T. E. Larson, *Am. Power Conf.* **35**, 678 (1963).
42. K. G. Baker, *Chem. Proc. Eng.* **56** (Jan. 1967).
43. C. H. Hosler, in C. H. Hosler, *Cooling Towers*, CEP Technical Manual, American Institute of Chemical Engineers, New York, 1972, p. 27.
44. D. B. Hoult, J. A. Fay, and L. J. Forney, *A Theory of Plume Rise Compared with Field Observations*, Fluid Mechanics Laboratory Publication No. 68-2, Massachusetts Institute of Technology, Department of Mechanical Engineering, Cambridge, Mass., 1968.
45. C. T. Karanoudis, Z. B. Maroulis, and D. Marinos-Kouris, *Chem. Eng. Res. Dev.* **72**, 307 (1994).
46. S. Simal, C. Rossello, and A. Berna, *Chem. Eng. Sci.* **49**(22), 3739 (1994).
47. M. C. Robbins and M. N. Ozisik, *Can. J. Chem. Eng.* **69**, 1262 (1991).
48. P. L. Douglas, J. A. T. Jones, and S. K. Mullick, *Chem. Eng. Res. Dev.* **72**, 325, 332, 341 (1994).
49. J. Chirife, *Adv. Drying* **2**, 73 (1983).
50. M. Mazzotti, G. Storti, and M. Morbidelli, *AIChE J.* **40**, 1825 (1994).
51. S. Joshi and J. R. Fair, *Ind. Eng. Chem. Res.* **27**, 2078 (1988).
52. B. A. Finlayson and L. C. Young, *AIChE J.* **25**, 192 (1979).
53. K. Zygourakis and R. Aris, *Chem. Eng. Sci.* **38**, 733 (1983).
54. D. C. Shallcross and S. L. Low, *Chem. Eng. Res. Dev.* **72**, 763 (1994).

General References

55. *Cooling Towers*, CEP Technical Manual, American Institute of Chemical Engineering, New York, 1972.
56. R. E. Treybal, *Mass Transfer Operations*, 2nd ed., McGraw-Hill Book Co., Inc., New York, 1968, 176–220.
57. A. S. Foust and co-workers, *Principles of Unit Operations*, 2nd ed., John Wiley & Sons, Inc., New York, 1980, Chapt. 17, 420–453.
58. D. W. Green and J. O. Maloney, *Perry's Chemical Engineers Handbook*, 6th ed., McGraw Hill Book Co., Inc., New York, 1984, 12–24.

59. E. J. Hoffman, *AIChE J.* **17**, 741 (1971).
60. A. S. H. Jernqvist, *Br. Chem. Eng.* **11**, 1205 (1966).
61. F. Kayihan, O. C. Sandall, and D. A. Mellichamp, *Chem. Eng. Sci.* **30**, 1333 (1975).
62. W. R. Lindberg and R. D. Haberstroh, *AIChE J.* **18**, 243 (1972).
63. J. L. Manganaro and O. T. Hanna, *AIChE J.* **16**, 204 (1970).
64. G. L. Standart, R. Taylor, and R. Krishna, *Chem. Eng. Commun.* **3**, 277 (1979).

LEONARD A. WENZEL
Lehigh University

Related Articles

Heat-exchange technology; Mass transfer; Engineering, chemical data correlation; Air conditioning; Evaporation